TWO APPROACHES FOR INCOHERENT PROPAGATION OF LIGHT IN RIGOROUS NUMERICAL SIMULATIONS

Andrej Campa[*]**, Janez Krc, and Marko Topic**

Faculty of Electrical Engineering, University of Ljubljana, Trzaska cesta 25, 1000 Ljubljana, Slovenia

Abstract—In multidimensional numerical simulations of optoelectronic devices the rigorous Maxwell equations are solved in different ways. However, numerically efficient incoherent propagation of light inside the layers has not been resolved yet. In this paper we present two time- and resource-efficient approaches for optical simulations of incoherent layers embedded in multilayer structures: (a) phase matching and (b) phase elimination approach. The approaches for simulating the incoherent propagation of light in thick layers are derived from Maxwell equations. Both approaches can be applied to any layer in the structure regardless of the position inside the structure and the number of incoherent layers. In rigorous simulations, for low absorbing thick layers scaling down the thickness and increasing extinction coefficient of the layer proportionally is implemented to shorten computational time. The simulation results are verified with the experiment on two types of structures: a bare glass incoherent layer and an amorphous silicon solar cell.

1. INTRODUCTION

Numerical simulations of optoelectronic devices using rigorous approaches, like finite element method (FEM), finite difference time domain (FDTD), finite integrating technique (FIT) or rigorous coupled wave analysis (RCWA) [1–5] in two- or three-dimensional space are getting more and more interest with the development of multiphysics software and extensive computer hardware. However, in rigorous optical simulations numerical solving of wave equation in frequency or time domain takes into account only coherent propagation of

electromagnetic waves (light). When simulating multilayer structures including one or more thick layers (thickness much larger than effective wavelength of light) one obtains dense large-amplitude interference fringes in simulated wavelength-dependent spectral characteristics of devices (e.g., reflectance, transmittance, absorptance), which are not observed in optical measurements. Absence of interference fringes in measured characteristics is linked to the following circumstances: the illumination is not an ideal monochromatic plane wave (there is lack in spatial and temporal coherence [6]); interfaces in the structure are not ideally flat and plan parallel. In thick layers this leads to so-called incoherent propagation of light if the thickness is larger than the correlation length [6], In thin layers, where thicknesses are in the range of light wavelengths, the propagation is still coherent, resulting in broad interference fringes, which are observed in measured spectral characteristics of thin-film solar cells [7, 8].

In case of thin-film silicon solar cells we often have very thick front glass superstrate (1–5 mm) as the carrier of the cell. Light propagates through the glass before reaching the thin cell. In order to avoid incoherent treatment of glass in rigorous simulations so far, the glass layer was simply omitted in simulations [9–11] or the glass, transparent conductive oxide, or Ethylene-vinyl acetate foil in case of substrate configuration, was often taken as incident medium [9, 12–15]. This, however, can lead to significant inaccuracy and uncertainty of the results since absorption in glass is fully neglected (in case of industrial glasses not always acceptable) and forward and backward reflectance at the front air/glass interface is not considered (in case of light scattering high incident angles of backward going light can result in total reflection at air/glass interface increasing light trapping), not to mention the incidence of light under oblique angles. In FDTD simulations the incorporation of an incoherent light source for different electromagnetic applications is possible [16, 17] however the simulations of solar cells/opto-electronic devices in the time domain may not be as accurate as in the frequency domain. In frequency domain the wavelength-dependent material parameters and solar illumination spectrum can be easily incorporated in simulations, resulting in very accurate simulations over broad wavelength region by splitting it to 5 or 10 nm step. Spectral averaging over the wavelength region is not acceptable since the interference fringes from thin layers should not be averaged. To average the interference fringes only in thick layers we would need additional series of simulations around specific wavelength(s), thus introducing large number of additional time-consuming simulations.

In this paper, we present an approach how to treat incoherent

propagation of light in a layer (thick or thin) in rigorous optical simulations. The approach is based on applying layer thickness adjustment(s) to manipulate with the phase of the reflected waves in order to eliminate interference fringes originating from the layer. Existing techniques, using Nyquist approximation, has been reported for the case of one-dimensional semi-coherent modeling for perpendicular incidence of light by [18] and later by [19] where four corrected thickness of an incoherent layer were used, resulting in four 1-D simulations and their averaging. Our approach for the case of rigorous two- and three-dimensional simulations is using (a) only one and (b) two thicknesses of an incoherent layer, compared to existing techniques. First the background theory and two models' development are presented. Then the models are employed in three-dimensional FEM simulations. Examples of simulations of a single layer thick glass and thick glass in a thin-film amorphous silicon solar cell are demonstrated.

2. THEORY AND TWO APPROACHES

Our aim is to eliminate dense interference fringes as a consequence of one or more thick layers in simulated structures, which should be treated incoherently. In first step we will assume some idealized conditions for the structures, later on we will extend the models to more realistic structures. First, we assume all interfaces in a plan parallel multilayer structure are flat. All the materials have isotropic optical properties and there is only one layer which we treat incoherently and has negligible absorption. Mathematically the incoherent approach can be applied to any layer regardless to its thickness.

The interference fringes that we want to eliminate in our model originate from interference effects in the layer i between the waves reflected from the top ($i1$) and the bottom interface ($i2$) of the incoherent layer (Figure 1). We assume a plane wave entering from the incident medium under angle θ into the first layer with a complex refractive index N_1. We define complex refractive index as $N = n - j\kappa$, where n in real refractive index and κ is extinction coefficient. Both are wavelength (λ) dependent in general.

$$\mathbf{E}_1(\mathbf{r}) = r_i \mathbf{E}_{inc}(r) = r_i \mathbf{E}_0 e^{jk_{i-1}\mathbf{r}} \tag{1}$$

$$\mathbf{E}_2(\mathbf{r}) = t_i^+ r_b t_i^- \mathbf{E}_0 e^{jk_{i-1}\mathbf{r} - jk_i 2d} \tag{2}$$

In (1) and (2) $\mathbf{E}_{inc}$ is the sum of forward-going light waves (forward means down in our case) with the same incident angle and is defined at the top of the interface ($i1$). $\mathbf{E}_0$ is its electric field amplitude, k_i is a wave number in media (i), t_i^+, t_i^- and r_i are Fresnel coefficients of
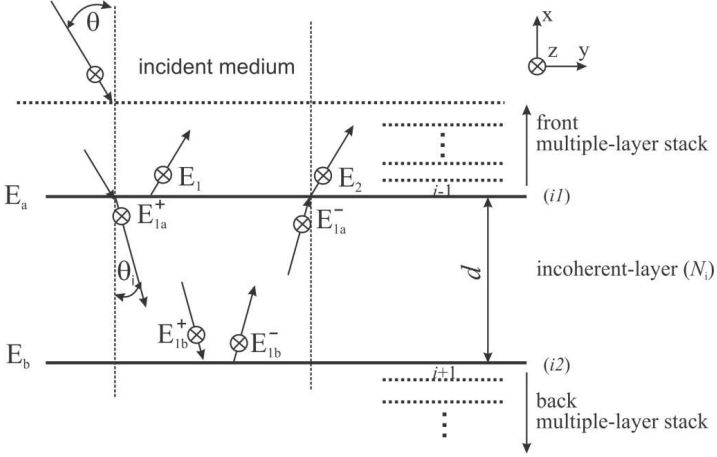
Figure 1. Propagation of plane waves in an incoherent layer embedded in multiple-layer structure.

transmittance and reflectance of interface $(i1)$, r_b is common reflectance coefficient of the complete stack at the bottom side of the incoherent layer (not only of the interface $(i2)$ of the incoherent layer), d_i is the thickness of the incoherent layer and $\mathbf{r}(x, y, z)$ is a position vector in a space inside layer $i - 1$. The electric field $\mathbf{E}$, representing the sum of backward going waves is determined as:

$$\mathbf{E}(\mathbf{r}) = \mathbf{E}_1(\mathbf{r}) + \mathbf{E}_2(\mathbf{r}) = r_i \mathbf{E}_0 e^{jk_{i-1}\mathbf{r}} + t_i^+ r_b t_i^- \mathbf{E}_0 e^{jk_{i-1}\mathbf{r} - jk_i 2d} \quad (3)$$

The corresponding power density (intensity), according to the Poynting theorem for the plane wave, is proportional to $\mathbf{E}\mathbf{E}^*$ (also to $\mathbf{H}\mathbf{H}^*$, however resulting in same rules about phases in equations following the Equation (4)):

$$
\begin{aligned}
\mathbf{E}\mathbf{E}^* &= \left(r_i \mathbf{E}_0 e^{jk_{i-1}\mathbf{r}} + t_i^+ r_b t_i^- \mathbf{E}_0 e^{jk_{i-1}\mathbf{r} - jk_i 2d} \right) \\
&\quad \cdot \left(r_i \mathbf{E}_0 e^{jk_{i-1}\mathbf{r}} + t_i^+ r_b t_i^- \mathbf{E}_0 e^{jk_{i-1}\mathbf{r} - jk_i 2d} \right)^* \\
&= \left| r_i^2 \right| \left| \mathbf{E}_0^2 \right| + \left| t_i^{+2} \right| \left| r_b^2 \right| \left| t_i^{-2} \right| \left| \mathbf{E}_0^2 \right| \\
&\quad + \left| r_i \right| \left| t_i^+ \right| \left| r_b \right| \left| t_i^- \right| \left| \mathbf{E}_0^2 \right| e^{jk_i 2d + j\varphi_i - j\varphi_i^+ - j\varphi_b - j\varphi_i^-} \\
&\quad + \left| r_i \right| \left| t_i^+ \right| \left| r_b \right| \left| t_i^- \right| \left| \mathbf{E}_0^2 \right| e^{-jk_i 2d - j\varphi_i + j\varphi_i^+ + j\varphi_b + j\varphi_i^-} \quad (4)
\end{aligned}
$$

φ_i and φ_b are the phase shifts due to reflectance at the interface $(i1)$ and at the back interface $(i2)$ including the bottom stack, respectively. They are equal to the phase of reflectance coefficients r_i and r_b which are complex numbers. The transmittance coefficients introduce phase shift (φ_i^+ and φ_i^-) only to the wave reflected from the bottom stack

$\mathbf{E}_2$. φ_i^+ and φ_i^- are phase shifts for forward and backward propagating waves at top interface ($i1$) of incoherent layer. The first two terms in (4) (third line) are related to the propagating waves with no interaction, while the last two terms (fourth and fifth line) are so-called interference terms [3]. The sum of last two terms is always real, applying the Euler's formula the imaginary parts cancel out. From the interference terms the maxima and minima of the intensity can be calculated. The constructive interference of the backward-going waves ($\mathbf{E}_1$, $\mathbf{E}_2$) is obtained if condition (5) is fulfilled:

$$2k_i d + \varphi_i - \varphi_i^+ - \varphi_b - \varphi_i^- = (2m+1)\pi \qquad (5)$$

This can happen if the thickness is

$$d = \frac{(2m+1)\pi - \varphi_i + \varphi_i^+ + \varphi_b + \varphi_i^-}{2k_i}, \text{ for } m = 0, \pm 1, \pm 2, \ldots \qquad (6)$$

The destructive interference is present if

$$2k_i d + \varphi_i - \varphi_i^+ - \varphi_b - \varphi_i^- = 2m\pi \qquad (7)$$

and the corresponding thickness

$$d = \frac{2m\pi - \varphi_i + \varphi_i^+ + \varphi_b + \varphi_i^-}{2k_i}, \text{ for } m = 0, \pm 1, \pm 2, \ldots \qquad (8)$$

For incoherent propagation of light the sum of interference terms in (4) has to be cancelled out [6].

$$|r_i|\,|t_i^+|\,|r_b|\,|t_i^-|\,|\mathbf{E}_0^2|\,e^{jk2d+j\varphi_i-j\varphi_i^+-j\varphi_b-j\varphi_i^-}$$
$$+ |r_i|\,|t_i^+|\,|r_b|\,|t_i^-|\,|\mathbf{E}_0^2|\,e^{-jk2d-j\varphi_i+j\varphi_i^++j\varphi_b+j\varphi_i^-} = 0 \qquad (9)$$

In the following we show two different approaches of calculating incoherent propagation of light in a layer, first one we assign to *phase matching approach* and the second one is an approach based on *eliminating the phase*.

2.1. Phase Matching Approach

The idea behind this approach is to determine a proper adjustment of the thickness d of the incoherent layer that the sum of interference terms is zero, (16). This new single thickness is different for each light wavelength, however we preserve only one simulation run for one (or more) incoherent layers. This approach is applicable if we know the reflectance coefficient r_b of the entire stack of layers after each incoherent layer. In case of flat interfaces this can be pre-calculated analytically, e.g., using transfer matrix method [20].

Due to simplicity reasons we are showing the model for 2-D domain with the propagation in xy-direction. With one coordinate extension the model is simply applicable to 3-D space. Equations (1) and (2) can be in 2-D space written as

$$
\begin{aligned}
E_1(x,y) &= E_1 = r_i E_0 e^{jk_{i-1x}x - jk_{i-1y}y} \\
E_2(x,y) &= E_2 = t_i^+ t_i^- r_b E_0 e^{jk_{i-1x}x - jk_{i-1y}y - jk_{ix}2d}
\end{aligned}
\tag{10}
$$

where k_{ix} and k_{iy} are the wavenumbers in the layer i in direction x and y, respectively.

$$
k_{ix} = k_i \cos(\theta_i) = N_i k_0 \cos(\theta_i) = \frac{2\pi}{\lambda} N_i \cos(\theta_i)
\tag{11}
$$

N_i is the complex and wavelength dependent refractive index and θ_i the angle of propagation in the layer i. λ is wavelength of light in free space. Equation (9) is simplified to

$$
|r_i|\,|t_i^+|\,|r_b|\,|t_i^-|\,|E_0^2|\,2\cos(k_{ix}2d + \varphi_i - \varphi_i^+ - \varphi_b - \varphi_i^-) = 0
\tag{12}
$$

The Equation (12) is reduced to zero when the argument in cosines function is zero, resulting in

$$
k_{ix}2d + \varphi_i - \varphi_i^+ - \varphi_b - \varphi_i^- = \frac{\pi}{2} + m\pi \text{ for } m = 0, \pm 1, \pm 2, \pm 3, \ldots
\tag{13}
$$

and the corresponding thickness

$$
d' = \mathrm{Re}\left[\frac{\frac{\pi}{2} + m\pi - \varphi_1 + \varphi_i^+ + \varphi_b + \varphi_i^-}{\frac{2\pi}{\lambda} N_i \cos(\theta_i) \cdot 2}\right] = \mathrm{Re}\left[\begin{array}{c}\frac{\lambda}{8N_i \cos(\theta_i)} + \frac{m\lambda}{4N_i \cos(\theta_i)} \\ + \frac{(\varphi_i^+ + \varphi_b + \varphi_i^- - \varphi_1)\lambda}{4\pi N_i \cos(\theta_i)}\end{array}\right]
\tag{14}
$$

for $m = 0, \pm 1, \pm 2, \pm 3, \ldots$

The new, adjusted thickness (d') needs to be determined according to Equation (14) for each wavelength. Parameter m should be selected in a way that d' is as close as possible to original d. Since the layers which we want to treat as incoherent are usually very thick with respect to the wavelength $(d \gg \lambda)$, shifting the thickness for some small Δ does not introduce noticeable error to the wave propagating through the incoherent layer and the absorption error is negligible.

$$
d' = d + \Delta, \quad \Delta \ll d
\tag{15}
$$

Only one simulation per wavelength is needed, however d' needs to be calculated in advance. This approach is not applicable whenever we have more complex structure beneath the incoherent layer (e.g., stack with textured interfaces as in the case of thin-film solar cells) and the r_b cannot be calculated analytically. Therefore we have developed the second approach.

2.2. Phase Elimination Approach

The interference term in Equation (4) can vanish indirectly by eliminating the phase shift introducing not only one but two adjusted thicknesses (resulting in two instead of one simulation per wavelength). The first simulation can be done at original thickness d, while the second simulation is calculated at thickness d'' which is obtained from canceling out the left side of Equation (12) which is non-zero in this case

$$\begin{aligned}
\cos(k_{ix}2d+\varphi_i-\varphi_i^+-\varphi_b-\varphi_i^-) &= -\cos(k_{ix}2d'+\varphi_i-\varphi_i^+-\varphi_b-\varphi_i^-) \\
&= \cos(k_{ix}2d'+\varphi_i-\varphi_i^+-\varphi_b-\varphi_i^- \pm m\pi) \text{ for } m=\pm 1,\pm 2,\dots \\
d'' &= d \pm \mathrm{Re}\left[\frac{m\pi}{2k_{ix}}\right] = d \pm \mathrm{Re}\left[\frac{m\lambda}{4N_i\cos(\theta_i)}\right]
\end{aligned} \tag{16}$$

Also here it is desired to take the closest thickness d'' to original thickness to minimize the absorption error, thus $m = 1$. The average of intensities of two simulations at thickness d and d'' gives the same results as phase matching therefore incoherent propagation of light inside the specific layer is taken into account. The second thickness d'' needs to be determined per wavelength. In following sections we will describe approximations that are needed if the model is applied to more realistic structures.

2.3. Including Very Thick Incoherent Layer in Rigorous Simulation

Very thick layers (in range of millimeters) are difficult to be included in rigorous simulations despite using adaptive meshing that some software packages offer. If the extinction coefficient of the incoherent layer (κ_i) is much smaller compared to the real part (n_i) of complex refractive index at wavelength of interest (e.g., $10000 * \kappa_i \ll n_i$; at $d = 1\,\mathrm{mm}$), we propose to include such incoherent layer in rigorous simulation in the following way. One scales down the thickness from millimeter to micrometer range (acceptable thickness for efficient rigorous simulation) and at the same time scales up the extinction coefficient of the material for the same factor. With this the absorption within the layer is preserved as shown in (17). However, with this we change the ratio between the wavelength in the layer and layer thickness, which in case of incoherent treatment of the layer is not important. According to Equations (4) and (8) the attenuation of the field in one pass for the incoherent propagation of light in the thick layer with original thickness d is proportional to

$$e^{\mathrm{Re}(-jk_id)} = e^{\mathrm{Re}(-jN_ik_0d)} = e^{-\kappa_ik_0d} \tag{17}$$

Since the incoherent propagation of light is not related to constructive and destructive interferences and attenuation is related only to (17), the scaling down the thickness of incoherent layer can be beneficial in order to reduce the number of elements of the model. In order to scale down the thickness of the layer we have to keep the Equation (17) constant. The new extinction coefficient κ_i^* at changed thickness d^* is

$$e^{-\kappa_i k_0 d} = e^{-\kappa_i^{*\prime} k_0 d^*} \Rightarrow \kappa_i^* = \frac{\kappa_i d}{d^*} \qquad (18)$$

If the condition $\kappa_i^* \ll n_i$ is fulfilled, the influence of the change in κ has negligible effect on reflectances and transmittances at the top and bottom interface of the incoherent layer.

2.4. Rough Surfaces

According to scalar scattering theory [21–24] the reflectance or transmittance at rough interface can be divided to the specular part and diffused part. Since diffused part of the light has usually a random nature (assuming randomly nano-rough interfaces), the phases of scattered light at different angles are random and thus the interference term is canceled for diffused light. However, the specular part of the light still remains the properties of a plane wave. Thus, both presented approaches can be used to eliminate the interference terms of specular part, where reflectance and transmittance are corrected Fresnel coefficients for specular light [25, 26].

3. RESULTS — APPLICATION OF THE MODELS

In this section, we apply the presented models to Subsection 3.1 a thick glass layer in air and Subsection 3.2 to a complete thin-film silicon solar cell. COMSOL Multiphysics® simulator, which is based on FEM, was used in our simulations [27]. Measured complex refractive indexes of layers were employed [26].

3.1. Single Glass Layer

The actual thickness of the microscope glass layer (Assistent) used in our experiment is 1 mm. Following Subsection 2.4 we scaled down the thickness to $d^* = d/1000 = 1\,\mu\text{m}$. κ' was scaled up at all discrete wavelengths for the same factor (1000). In the wavelength region $\lambda = 300$–$900\,\text{nm}$ where we run simulations it holds $\kappa^* \ll n_{\text{glass}}$.

Real and imaginary part of the measured complex refractive index of glass used in simulations is shown in Table 1 for selected wavelengths.

Table 1. Complex refractive index of the microscope glass.

Wavelength [nm]	n_{glass}	κ_{glass}
350	1.558	6.787×10^{-7}
360	1.556	2.032×10^{-7}
370	1.552	3.616×10^{-8}
385	1.549	1.586×10^{-8}
400	1.545	0
500	1.529	0
600	1.520	0
700	1.516	0
900	1.519	0
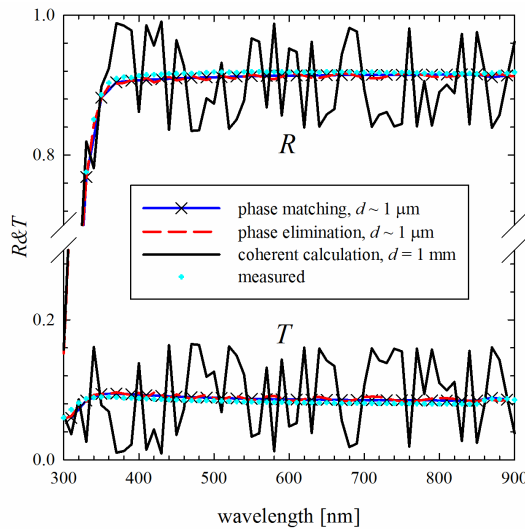
Figure 2. Comparison of measured (symbols) and simulated reflectance and transmittance obtained by coherent calculation (black line), phase matching approach (blue line) and phase elimination approach (red line).

The COMSOL model of glass layer surrounded by air was built in 3-D (although it is 1-D problem). The reflectance and transmittance from glass layer was measured with PerkinElmer Lambda 950 spectrophotometer in the range between 300 nm to 900 nm with the wavelength step of 10 nm. The default setting for slit width in the instrument is narrow enough to obtain coherent propagation in thin layers and incoherent propagation of light in thick layers in

our case of glass layer. Simulations were carried out in the same
wavelength range and with the same wavelength step. Figure 2, shows
good agreement between the measured values and calculated curves
for reflectance and transmittance for both incoherent approaches. The
values were calculated first by the *phase matching approach* (blue
line) where the phases were determined analytically from the Fresnel
equations assuming perpendicular incidence of light $\theta = 0$, thus

$$\varphi_i = \pi \quad \varphi_b = \varphi_i^+ = \varphi_i^- = 0 \tag{19}$$

From (14) the actual thickness can be chosen from

$$d'(\lambda) = \frac{\lambda}{8n_{\text{glass}}(\lambda)} + \frac{m\lambda}{4n_{\text{glass}}(\lambda)} - \frac{\lambda}{4n_{\text{glass}}(\lambda)} \tag{20}$$

The m was selected for each wavelength in such a manner that the
new thickness was close to scaled original thickness ($1\,\mu$m), e.g., $m = 21$
at $\lambda = 300\,$nm, $d' = 976.3\,$nm and $m = 7$ at $\lambda = 900\,$nm, $d' = 962.6\,$nm.
The second approach used was the *phase elimination approach* (red
dashed line, Figure 2) and it requires 2 thicknesses. The first thickness
was fixed to $1\,\mu$m and the second thickness d'' was calculated according
to Equation (16) to

$$d'' = 1\,\mu\text{m} + \frac{\lambda}{4n_{\text{glass}}} \tag{21}$$

(at $\lambda = 300\,$nm $d'' = 1047.6\,$nm and at $\lambda = 900\,$nm $d'' = 1148.1\,$nm).
In both cases the κ_{glass}^* was modified according to (18). For both
approaches very good agreement in reflectance and transmittance is
obtained compared to measured values. Additionally to the incoherent
propagation of light, the coherent propagation of light was simulated
for $1\,$mm thick glass layer (black line). Due to large wavelength step
of $10\,$nm high density of the interferences is not reproduced well in its
full extend. However, the coherent simulation shows many interference
fringes as expected according to (4) [6].

3.2. Single-junction a-Si:H Solar Cell

To show the use of presented approaches in real photovoltaic
structures, we applied the second approach to single-junction thin-film
hydrogenated amorphous silicon (a-Si:H) solar cell (Figure 3). The
structure of the simulated cell is shown in Figure 3, the top contact
(looking from incidence of light) is consisted of $650\,$nm thick SnO_2:F
transparent conductive oxide layer (commercially available Asahi U
type), with the random pyramid like nano-roughness structure at the
bottom interface. The a-Si:H cell is built on top of the rough SnO_2:F
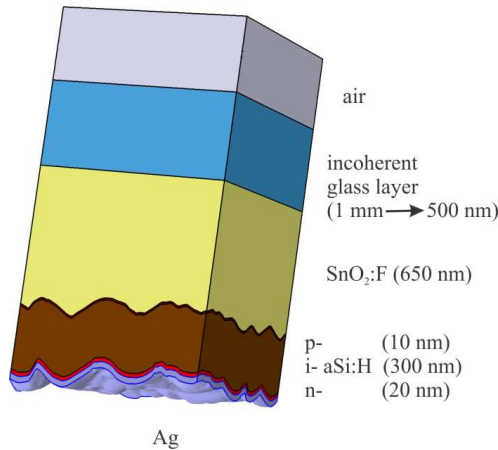layer, with the $10\,$nm doped p-layer followed by $300\,$nm thick intrinsic

Figure 3. Simulated structure of single-junction a-Si:H Solar cell.

a-Si:H layer and 20 nm thick doped n-layer of amorphous silicon and finalized with a back contact made of silver (Ag). Ag layer thickness in simulations was 50 nm followed by absorbing boundary condition, since this combination is equivalent to a thick Ag layer. The solar cell quantum efficiency was measured using Xe lamp with monochromator in the range between 400 and 800 nm and with the step of 10 nm. The width of entrance and exist slits of monochromator should not be too wide in order to obtain coherent propagation of light in thin layers.

Due to light scattering at random rough interfaces it is practical only to apply the second approach based on *phase elimination* (2.2). It is very hard to determine the exact phase values needed in *phase matching approach*, thus we have used the *phase eliminating approach* to perform simulations.

The two modified and scaled down thicknesses of glass layer used in simulations were 500 nm (factor 2000) and the second thickness was

$$d'' = 500\,\text{nm} - \frac{\lambda}{4n_{\text{glass}}(\lambda)} \qquad (22)$$

The results were calculated by taking the average of absorptance of both simulations.

The simulation was done between wavelengths 400 and 800 nm with the wavelength step size of 10 nm, Figure 4. In a-Si:H solar cells, the measured quantum efficiency can be directly compared to the absorptance in i-layer, considering ideal extraction of charge carriers from the i-layer and neglecting the contribution from defect-rich p- and n-layer [8]. Good agreement is obtained between measured quantum
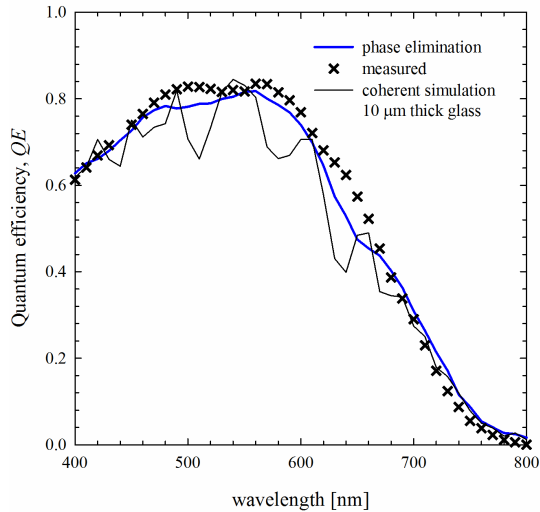
Figure 4. Comparison of measured (symbols) Quantum efficiency of a-Si:H solar cell and simulated Quantum efficiency by phase elimination approach (blue line) and with coherent calculation of 10 μm thick glass (black line).

efficiency (symbols) and simulated absorptance in i-layer obtained by the *phase elimination approach* (blue line). Additionally, solar cell with the coherent propagation of light was simulated for 10 μm thick glass layer (black line). The coherent simulation shows the expected interference fringes. Due to the high glass thickness (1 mm) we could not perform the simulation of the complete thick glass layer. The 10 μm thick glass layer shows only few interferences and for a thicker layer more interferences are expected as in the case presented in Subsection 3.1.

4. DISCUSSION

Both presented approaches, the *phase eliminating* (2.1) and *phase matching approach* (2.2), works very well for more incoherent layers. The procedure is the same as described before. At the phase matching approach (2.1) we have to calculate the phase difference for all incoherent layers, adjust all thicknesses and then carry out only one simulation per wavelength. However, finding the phase can be difficult, thus in this cases the *phase eliminating approach* (2.2) can be used. For this approach all incoherent layers have to be simulated two times

in order to eliminate the interference fringes. In the case of more than one incoherent layer all possible combinations have to be taken into account, thus the number of needed simulations is 2^m where m is number of incoherent layers. This is still much less than the approaches published so far where 4^m simulations are needed.

Both models are sensitive to numerical phase error that is present in rigorous numerical simulations. Phase error per wavelength is dependent on discretization and element order [28]. For finer discretization the phase error is lower. In order to keep the discretization size of the incoherent layer in reasonable large size we have to thin down very thick incoherent layer(s). The thicker layers of few wavelengths have higher phase error compared to thinner layers with the same discretization size. Also the first approach of *phase matching* is more sensible to this discretization error compared to *phase eliminating approach*. The possible reason for this is the *phase eliminating approach* is comparing two layers that are close together with the thicknesses (14), and the phase error is more or less the function of the difference. While in the *phase matching approach* the phase error is related to the whole thickness of incoherent layer. The *phase eliminating approach* is partly eliminating also the phase error due to discretization for the common part of the thickness, but only when the discretization is similar for both thicknesses. In simulation of incoherent glass layer we had to take finer discretization step for *phase matching approach* to achieve comparable results to the *phase eliminating approach* with larger discretization step. The discretization step in incoherent layer was around 3 times finer for *phase matching approach*, results are not shown here.

5. CONCLUSION

In the presented work, we have showed two very efficient approaches to take into account the incoherent layers in the rigorous coherent simulations. The *phase matching approach* needs only one simulation run, however analytical determination of the required phase might be too challenging. Thus, the second approach of phase elimination is much more appropriate. Two simulation runs for one incoherent layers per wavelength are needed. However, the thicknesses determination is straightforward. Both approaches are much more efficient to the existing method using Nyquist approximation. The models were tested on two different structures, one on a glass layer and the second one on the realistic structure of thin-film silicon solar cell. In both cases very good agreement between measurements and simulations is observed.

REFERENCES

1. Jin, J.-M., *The Finite Element Method in Electromagnetics*, 2nd Edition, Wiley-IEEE Press, 2002.

2. Moharam, M. G. and T. K. Gaylord, "Rigorous coupled-wave analysis of planar-grating diffraction," *J. Opt. Soc. Am.*, Vol. 71, No. 7, 811–818, 1981.

3. Fotyga, G., K. Nyka, and M. Mrozowski, "Efficient model order reduction for FEM analysis of waveguide structures and resonators," *Progress In Electromagnetics Research*, Vol. 127, 277–295, 2012.

4. Klopf, E. M., S. B. Manić, M. M. Ilić, and B. M. Notaroš, "Efficient time-domain analysis of waveguide discontinuities using higher order FEM in frequency domain," *Progress In Electromagnetics Research*, Vol. 120, 215–234, 2011.

5. Guo, X.-M., Q.-X. Guo, W. Zhao, and W. Yu, "Parallel FDTD simulation using NUMA acceleration technique," *Progress In Electromagnetics Research Letters*, Vol. 28, 1–8, 2012.

6. Born, M. and E. Wolf, *Principles of Optics*, 7th Edition, Cambridge University Press, Cambridge, 1999.

7. Rau, U., D. Abou-Ras, and T. Kirchartz, *Advanced Characterization Techniques for Thin Film Solar Cells*, Wiley, Weinheim, 2011.

8. Krc, J., M. Zeman, O. Kluth, F. Smole, and M. Topic, "Effect of surface roughness of ZnO:Al films on light scattering in hydrogenated amorphous silicon solar cells," *Thin Solid Films*, Vol. 426, Nos. 1–2, 296–304, 2003.

9. Solntsev, S. and M. Zeman, "Optical modeling of thin-film silicon solar cells with submicron periodic gratings and nonconformal layers," *Energy Procedia*, Vol. 10, No. 0, 308–312, 2011.

10. Campa, A., J. Krc, and M. Topic, "Analysis and optimisation of microcrystalline silicon solar cells with periodic sinusoidal textured interfaces by two-dimensional optical simulations," *Journal of Applied Physics*, Vol. 105, No. 8, 083107, 2009.

11. Isabella, O., A. Campa, M. Heijna, W. J. Soppe, A. J. M. van Erven, R. H. Franken, H. Borg, and M. Zeman, "Diffraction gratings for light trapping in thin-film silicon solar cells," *23rd European*

Photovoltaic Solar Energy Conference and Exhibition, 2320–2324, Valencia, Spain, 2008.

12. Haase, C. and H. Stiebig, "Optical properties of thin-film silicon solar cells with grating couplers," *Progress in Photovoltaics: Research and Applications*, Vol. 14, No. 7, 629–641, 2006.

13. Lipovsek, B., M. Cvek, A. Campa, J. Krc, and M. Topic, "Analysis and optimisation of periodic interface textures in thin-film silicon solar cells," *25th European Photovoltaic Solar Energy Conference and Exhibition*, 3120–3123, Valencia, Spain, 2010.

14. Dewan, R., I. Vasilev, V. Jovanov, and D. Knipp, "Optical enhancement and losses of pyramid textured thin-film silicon solar cells," *Journal of Applied Physics*, Vol. 110, No. 1, 013101–013101-10, Jul. 2011.

15. Jandl, C., K. Hertel, C. Pflaum, and H. Stiebig, "Simulation of silicon thin-film solar cells for oblique incident waves," *25th European Photovoltaic Solar Energy Conference and Exhibition*, 806505, Valencia, Spain, 2011.

16. Choi, W. J., Q.-H. Park, D. Kim, H. Jeon, C. Sone, and Y. Park, "FDTD simulation for light extraction in a GaN-based led," *Journal of the Korean Physical Society*, Vol. 49, No. 3, 877–880, 2006.

17. Capoglu, I. R., C. A. White, J. D. Rogers, H. Subramanian, A. Taflove, and V. Backman, "Numerical simulation of partially coherent broadband optical imaging using the finite-difference time-domain method," *Optic Letters*, Vol. 36, No. 9, 1596–1598, 2011.

18. Stiebig, H., "Entwicklung und beschreibung von optoelektronis-chen bauelementen auf der basis amorphen siliziums," Ph.D. Thesis, Berichte des Forschungszentrums Jülich, Jülich, 1997.

19. Krc, J., "Analysis and modelling of thin-film optoelectronic structures based on amorphous silicon," Ph.D. Thesis, University of Ljubljana, Ljubljana, 2003.

20. Martin-Palma, R. J., J. M. Martinez-Duart, and A. Macleod, "Determination of the optical constants of a semiconductor thin film employing the matrix method," *IEEE Transactions on Education*, Vol. 43, No. 1, 63–68, 2000.

21. Beckmann, P. and A. Spizzichino, *The Scattering of Electromagnetic Waves from Rough Surfaces*, Artech Print on Demand, 1987.

22. Bennett, H. E. and J. O. Porteus, "Relation between surface roughness and specular reflectance at normal incidence," *J. Opt. Soc. Am.*, Vol. 51, No. 2, 123–129, 1961.

23. Porteus, J. O., "Relation between the height distribution of a rough surface and the reflectance at normal incidence," *Journal of the Optical Society of America*, Vol. 53, No. 12, 1394, 1963.

24. Carniglia, C. K., "Scalar scattering theory for multilayer optical coatings," *Optical Engineering*, Vol. 18, 104–115, 1979.

25. Krc, J., F. Smole, and M. Topic, "Analysis of light scattering in amorphous Si:H solar cells by a one-dimensional semi-coherent optical model," *Progress in Photovoltaics: Research and Applications*, Vol. 11, No. 1, 15–26, 2003.

26. Springer, J., A. Poruba, and M. Vanecek, "Improved three-dimensional optical model for thin-film silicon solar cells," *Journal of Applied Physics*, Vol. 96, No. 9, 5329, 2004.

27. Multiphysics Modeling and Simulation Software, Available: http://www.comsol.com/.

28. Warren, G. S. and W. R. Scott, "Numerical dispersion in the finite-element method using three-dimensional edge elements," *Microwave and Optical Technology Letters*, Vol. 18, No. 6, 423–429, 1998.